

Antioxidant activity from inactivated yeast: Expanding knowledge beyond the glutathione-related oxidative stability of wine



Florian Bahut^a, Rémy Romanet^a, Nathalie Sieczkowski^b, Philippe Schmitt-Kopplin^{c,d},
Maria Nikolantonaki^{a,*}, Régis D. Gougeon^a

^a Univ. Bourgogne Franche-Comté, AgroSup Dijon, PAM UMR A 02.102, Institut Universitaire de la Vigne et du Vin – Jules Guyot, F-21000 Dijon, France

^b Lallemand SAS, 19 rue des Briquetiers, BP 59, 31 702 Blagnac, France

^c Research Unit Analytical BioGeoChemistry, Helmholtz Zentrum München, Ingolstaedter Landstrasse 1, 85764 Neuherberg, Germany

^d Chair of Analytical Food Chemistry, Technical University of Munich, Alte Akademie 10, D-85354 Freising, Germany

ARTICLE INFO

Keywords:

Oxidative stability
Glutathione
Nucleophile
Wine
Chardonnay

Chemical Compounds:

4-Methylcatechol (PubChem CID9958)
Hydrogen sulfide (PubChem CID402)
Acetaldehyde (PubChem CID177)
Sulfite (PubChem CID1099)
Hexanal (PubChem CID6184)
Cysteine (PubChem CID5862)
Isopentylacetamide (PubChem CID263768)
Cysteinyl-glycine (PubChem CID439498)
Hydroxydecanoic acid (PubChem CID21488)
Glutamyl-cysteine (PubChem CID10171468)
Glutathione (PubChem CID124886)

ABSTRACT

Maintaining wine oxidative stability during barrel ageing and shelf life storage remains a challenge. This study evaluated the antioxidant activities of soluble extracts from seven enological yeast derivatives (YDs) with increased glutathione (GSH) enrichment. YDs enriched in GSH appeared on average 3.3 times more efficient at quenching radical species than YDs not enriched in GSH. The lack of correlation (Spearman correlation $\rho = 0.46$) between the GSH concentration released from YDs and their radical scavenging activity shed light on other non-GSH compounds present. After 4-methyl-1,2-benzoquinone derivatization, UHPLC–Q-ToF MS analyses specifically identified 52 nucleophiles potentially representing an extensive molecular nucleophilic fingerprint of YDs. The comparative analysis of YD chemical oxidation conditions revealed that the nucleophilic molecular fingerprint of the YD was strongly correlated to its antiradical activity. The proposed strategy shows that nucleophiles co-accumulated with GSH during the enrichment of YDs are responsible for their antioxidant activities.

1. Introduction

Early oxidation by nonenzymatic reactions could affect wine quality and thus its economic value. The natural occurrence of transition metals in wine is thought to initiate metal-catalyzed reduction of oxygen, leading to generate hydroperoxyl radicals, which are highly reactive radical oxygen species (ROS), and polyphenol-derived quinones (Danilewicz, 2003). The hydroperoxyl radical reacts quickly and non-selectively with ethanol in wine to yield 85% of 1-hydroxyethyl radical (Elias et al., 2009). The latter is then involved in further chemical

reactions with main wine compounds, such as phenols or thiols, resulting in color browning and varietal aroma loss, which are key attributes of wine organoleptic quality, in particular for white wines (Kreitman, Laurie, & Elias, 2013; Li, Guo, & Wang, 2008; Nikolantonaki & Waterhouse, 2012). The genuine antioxidant composition of the wine (phenolic compounds, sulfhydryl compounds, organic acids) regulates the oxidation rate and thus the shelf-life of the wine (Kontogeorgos & Roussis, 2014). In order to preserve wine longer, sulfur dioxide (SO₂) is one of the most versatile and efficient wine antioxidants used to prevent early oxidation. However, intolerances caused by SO₂ derivatives have

Abbreviations: 4MeC, 4-methylcatechol; 4MeQ, 4-methyl-1,2-benzoquinone; DPPH, 2,2-diphenyl-1-picrylhydrazyl; ESI, electrospray ionization; FTICR-MS, Fourier-transform ion cyclotron resonance mass spectrometry; LOD, limit of detection; *m/z*, mass/charge; PCA, principal component analysis; Rm_{20%}, mass ratio to reduce 20% initial absorbance; RT, retention time; SO₂, sulfur dioxide (sulfite); *t*_{1/2}, half-life constant; UHPLC–Q-ToF-MS, ultra-high-performance liquid chromatography coupled to quadrupole time-of-flight mass spectrometer; YD, yeast derivative

* Corresponding author at: Université de Bourgogne, UMR PAM, 2 rue Claude Ladrey, 21000 Dijon, France.

E-mail address: maria.nikolantonaki@u-bourgogne.fr (M. Nikolantonaki).

<https://doi.org/10.1016/j.foodchem.2020.126941>

Received 23 January 2020; Received in revised form 23 April 2020; Accepted 28 April 2020

Available online 30 April 2020

0308-8146/ © 2020 Elsevier Ltd. All rights reserved.

led to the reduction of its concentration in wines. In a competitive global winemaking market strategy, it is crucial to reduce or even eliminate the use of SO₂ as a preservative and to search for new healthier and safer strategies.

Yeast derivatives (YDs) applied biotechnology was proposed a decade ago, as a new strategy to control wine oxidation during bottle storage through oxygen consumption and release of antioxidants (Comuzzo et al., 2015; Pozo-Bayon, Andujar-Ortiz, & Moreno-Arribas, 2009). Indeed, YDs refer to a class or fraction of yeasts produced on an industrial scale as additives (Pozo-Bayon et al., 2009). Depending on the industrial process, YDs can be found under the form of inactivated yeast, yeast autolysate, yeast protein extract, yeast cell wall and yeast mannoprotein (Comuzzo et al., 2012; Pozo-Bayon et al., 2009).

Amongst the numbers of compounds released by YDs in wine, glutathione (GSH) receives most of the scientific attention (Bahut et al., 2019; Kritzinger, Bauer, & Du Toit, 2013). This tripeptide containing a cysteine residue is well known to be present naturally in grapes, wine and yeasts. The reductive property supported by the free sulfhydryl enables it to have various beneficial effects during wine aging. GSH has the ability to form colorless products which delay the browning of model white wine under accelerated oxidative conditions (Sonni et al., 2011). In addition, GSH exhibited a protective effect on aromas during aging, notably volatiles esters and terpenes (Papadopoulou & Roussis, 2008) and volatile thiols, and also reduced atypical flavors (Dubourdieu & Lavigne, 2004). In parallel, inactivated yeast rich in GSH showed stabilization of wine varietal aromas, such as volatile thiols and terpenes (Gabrielli, Aleixandre-Tudo, Kilmartin, Sieczkowski, & du Toit, 2017). Interestingly this study showed that pure GSH at the same concentration as the one released by inactivated yeast had a lower impact, notably on volatile thiols preservation. The combination of GSH with wine antioxidants (phenolic compounds and sulfites at different doses) has shown a positive impact on volatile compounds in long-term wine storage when compared with the use of sulfites alone (Roussis, Patrianakou, & Drossiadis, 2013). These results allowed us to hypothesize that the complex chemical composition brought into the must during fermentation by YDs could enhance the formation and/or the stabilization potential of wine aroma at the end of the fermentation.

According to a recent study on Chardonnay aged wines, Fourier-transform ion cyclotron resonance mass spectrometry (FTICR-MS) based metabolomics along with multivariate statistical analyses provided evidence that the GSH efficiency against oxidation during bottle aging is dependent on the wine's global antioxidant metabolome, including in particular N- and S-containing compounds like amino acids, aromatic compounds and peptides. These compounds possess a strong nucleophilic character and their reactivity with wine electrophiles, such as oxidized polyphenols, suggests the formation of stable adducts possessing lower oxidative potential (Nikolantonaki et al., 2018). YDs rich in GSH are thus gaining interest since they are a natural way for winemakers to increase the concentration of reduced GSH during winemaking and pre-bottling without direct addition of GSH, which is not yet allowed by European food additives regulations.

However, many of these studies about the impact of YDs on wine stability agree to highlight the combined effect of GSH with other compounds released by YDs. Indeed, the metabolic changes related to GSH accumulation in yeast can subsequently impact the diversity of metabolites released by YDs (Bahut et al., 2019). The objective of the present study was to characterize the antiradical effect of different YD products and to give insights into their chemical composition. This work constitutes a primary approach in understanding the action mechanisms of YDs and in establishing better criteria for their use in winemaking. Essentially, no study has shown a clear relationship between the diversity of compounds released by YDs and the potential oxidative stability of wine or other beverages. Our study is dedicated to exploring the stabilization potential properties of different yeast derivatives with a particular emphasis on the non-GSH soluble molecular fraction released in wine-like acidic medium.

2. Materials and methods

2.1. Chemicals

The water used in this study was ultrapure water (18.2 M Ω ; Millipore, Germany). Ethanol was purchased from Honeywell (United States); formic acid (MS grade), 2,2-diphenyl-1-picrylhydrazyl (DPPH), citric acid, 4-methylcatechol (4MeC) and phosphate dibasic from Sigma-Aldrich (St. Louis, MO). Methanol (MS grade and HPLC grade) and acetonitrile (MS grade) were purchased from Biosolve Chimie (Dieuze, France). FeSO₄·7H₂O (99,5%) was purchased from Carlo Erba (Milan, Italy)

2.2. Sample sets

Seven yeast derivatives produced on a laboratory scale were used for this study, labeled YD1 to YD4 and YD6 to YD8 (Supplementary Information 1). Each yeast derivative was mixed at 1 g/L in hydro alcoholic solution (12% (v/v) of ethanol with 0.01% (v/v) of formic acid to reach a pH of 3.2) previously deoxygenated by bubbling nitrogen through for 10 min. After an hour of stirring at room temperature and in the dark with a rotary stirrer, samples were centrifuged (15 min at 9000g at 10 °C) and the supernatants were separated and kept at 4 °C until analysis (Bahut et al., 2019). All samples were prepared freshly and analyzed within 24 h to prevent deterioration.

2.3. DPPH radical scavenging activity

The DPPH assay was performed following the protocol previously described (Romanet et al., 2019). A solution of 2,2-diphenyl-1-picrylhydrazyl (DPPH) was prepared by mixing 27 mg of DPPH with 1L of 60:40 (v/v) 0.3 M buffer citrate-phosphate:methanol to reach a pH of 3.6. In the absence of oxygen, 3.9 mL of the DPPH solution were mixed with 0.1 mL of sample at different mass ratio YD/DPPH (Rm). After 4-h incubation in darkness, sample absorbance was measured in a UV-Vis spectrometer at 525 nm. Absorbance was normalized with the blank (buffer with 0.1 mL of model wine). Results were expressed as the Rm needed to reduce the initial absorbance by 20%, designated Rm_{20%} and translated into the equivalent YD mass to provide the Rm_{20%} (calculation details in Supplementary Information 2).

2.4. Nucleophilic compounds derivatization

The derivatization was performed using an adaptation of the protocol described by Nikolantonaki and collaborators (Nikolantonaki & Waterhouse, 2012; Romanet, Bahut, Nikolantonaki, & Gougeon, 2020). Firstly, the freshly prepared quinone, 4-methyl-1,2-benzoquinone (4MeQ), is added to 1 mL of sample in excess concentration (final concentration 4MeQ is 1 mM). After 30 min of reaction at room temperature, 1.5 mM SO₂ is added to reduce the remaining 4MeQ in the sample. The addition of quinone in excess allows all nucleophilic compounds present in the soluble fraction of the yeast derivatives to be derivatized. A second set of analyses was performed by adding limiting amounts of 4MeQ, in order to derivatize compounds with the highest affinity for quinone. Six different limiting concentrations (from 30 μ M to 625 μ M) were added to samples for 30 min before quenching the reaction by addition of 1.5 mM of SO₂. Samples were then analyzed by high resolution UHPLC-Q-ToF-MS in positive and negative modes with the protocol described below.

2.5. High resolution UHPLC-Q-ToF MS(/MS) analysis

The separation was performed with an ultra-high-pressure liquid chromatography system (Dionex Ultimate 3000; ThermoFisher) coupled to a MaXis plus MQ ESI-Q-TOF mass spectrometer (Bruker, Bremen, Germany). The non-polar and low polar metabolites were

separated through reverse-phase liquid chromatography (RP-LC) by injecting 5 μL in an Acquity BEH C_{18} 1.7 μm column, 100 \times 2.1 mm (Waters, Guyancourt, France). Elution was performed at 40 $^{\circ}\text{C}$ using (A) acidified water (0.1% (v/v) formic acid) and (B) acetonitrile (0.1% (v/v) formic acid) with the following gradient: isocratic step from 0 to 1.10 min with 5% (v/v) B, then the percentage of B was increased to 95% (v/v) until 6.40 min, held there for 3 min and finally returned to the initial condition in 0.1 min for 5 min of re-equilibration. The flow rate was set to 400 $\mu\text{L min}^{-1}$. Electrospray and mass spectrometer acquisition parameters for positive and negative polarity are summarized in [Supplementary Information 3](#). A divert valve was used to inject four times diluted ESI-L Low Concentration Tuning Mix (Agilent, Les Ulis, France) at the beginning of each run, allowing a recalibration of each spectrum. The mass spectrometer was calibrated with undiluted Tuning Mix before batch analysis in enhanced quadratic mode, with less than 0.5 ppm errors after calibration. Acquisitions were done in the m/z 100 to 1500 mass range in positive ionization mode. Quality control was used to guarantee the stability of the UHPLC-Q-ToF MS system before each run. Calibrated ions were restricted to those with S/N better than 30 and an absolute intensity of at least 1000. Before features extraction (couple of m/z values and retention time), the spectral background noise was removed. The extracted features were aligned with an in-house R script with a maximum m/z tolerance of 3 ppm and retention time tolerance of 0.5 min and variables absent from more than 80% of the samples were removed from the analysis.

Features fragmentation was performed using the Scheduled Precursors List MS/MS function. The fragmentation was performed at two different collision energies: 20 and 35 eV. Parent ions and fragments were submitted to different databases through the massTRIX interface (<http://masstrix.org>) (Suhre & Schmitt-Kopplin, 2008) and YMDB 2.0 (<http://www.ymdb.ca>) and both compositional (obtained isotopic profile) and structural information were used to annotate compounds with high confidence level.

2.6. Chemical oxidation monitoring

The monitoring of chemical oxidation reactions was performed by UHPLC-Q-ToF MS analysis in negative mode using analytical conditions as described in [Section 2.5](#), with the temperature of the auto-sampler set to 30 $^{\circ}\text{C}$. Chemical oxidation was initiated by mixing 1 mL of YD soluble fraction at 1 g/L with 50 μL of 4MeC (20 mM) and 5 μL of $\text{FeSO}_4 \cdot 7\text{H}_2\text{O}$ (18 mM). Oxidation reactions were monitored after 5 min, and then every 50 min up to 40 h after initiation. Samples were analyzed in triplicate.

2.7. Data analysis

All experiments were performed at least in triplicate and if not specified, results were expressed as average \pm standard deviation for the triplicate. The basic data mining and data visualization were performed with R software v. 3.5.1. Nonparametric Kruskal-Wallis rank sum tests and Spearman tests were used for median comparison and correlation estimation, respectively. Curve fitting was performed with OriginPro 2017 (b.9.4.0.220).

After alignment, features that were positively correlated (Spearman correlation, $\rho > 0.1$) with the addition of the quinone were extracted. They were considered to be associated with compounds which had reacted with quinones. The nucleophile-quinone derivative is the result of the combination of $n^*4\text{MeC}$ ($1 \leq n$) with m^* nucleophiles ($1 \leq m \leq n + 2$) leading to $m^*\text{Nu} + n^*4\text{MeC}$ addition products (Ma, Bueschl, Schuhmacher, & Waterhouse, 2019). Thus, a specific $m^*\text{Nu} + n^*4\text{MeC}$ derivative carrying the m/z information of the corresponding free nucleophile and the combination of all the derivatives will be used to further express the nucleophilic fingerprints of the YDs. The SmartFormula tool from the DataAnalysis software (v.4.3, Bruker, Germany) allows attribution of a raw formula based on the detected m/z

and the isotopic profile ([Supplementary information 5](#)). Since sulfites were used to quench the derivatization reaction, nucleophilic addition of $x^*\text{HSO}_3^-$ ($0 \leq x$) on 4MeC moiety can be observed to form the nucleophilic addition product $m^*\text{Nu} + n^*4\text{MeC} + x^*\text{HSO}_3^-$. The putative raw formula (and thus the corresponding neutral mass) of the free nucleophiles was calculated by subtracting the raw formula of $n^*4\text{MeC} + x^*\text{HSO}_3^- - 2^*(n + x + m - 1)^*\text{H}$ from the total raw formula of the quinone derivative. The resulting nucleophile neutral formula was submitted to a database search (Metlin and YMDB) for putative annotation.

3. Results and discussions

3.1. Radical scavenging activity

The measurement of radical scavenging activity was firstly applied to estimate antioxidant properties of pure compounds or mixtures. The radical scavenging activity of the different YD soluble fractions was measured using the DPPH assay ([Fig. 2](#)), recently adapted for wine-like media (Romanet et al., 2019). DPPH is a stable radical in solution with a difference in absorbance between the radical and the protonated form. The decrease of the absorbance can be related to the protonation of the DPPH. It is thus possible to follow the reduction potential of a compound (or a mixture of compounds) with the amount/volume of sample needed to reduce the initial absorbance to a specific range ([Supplementary Information 2](#)).

[Fig. 1](#) shows the mass needed from different YDs to get a 20% decrease (mass equivalent) of the initial absorbance of the DPPH solution. The results of the DPPH assay allowed the following classification of YDs soluble fractions, going from the highest scavenging activity to the lowest: YD8 > YD7 > YD3 > YD1 > YD4 > YD6 > YD2. All tested YDs could reduce the DPPH radical, with YDs rich in GSH (YD8, YD7 and YD3) having the highest antiradical capacity compared to those without GSH accumulation. This result clearly demonstrated the wide range of potential antioxidant properties among the different YDs, with YD8 exhibiting nearly 10 times higher efficiency than YD2.

It is important to mention that only soluble fractions were used in this assay (insoluble fractions were removed by centrifugation). Thus, these results represent only a part of the antioxidant potential of the product (except for YD4, which was totally soluble). Indeed, it is known that insoluble fractions also have antioxidant activity, notably due to sulfur-containing compounds present in cell walls and mannoproteins

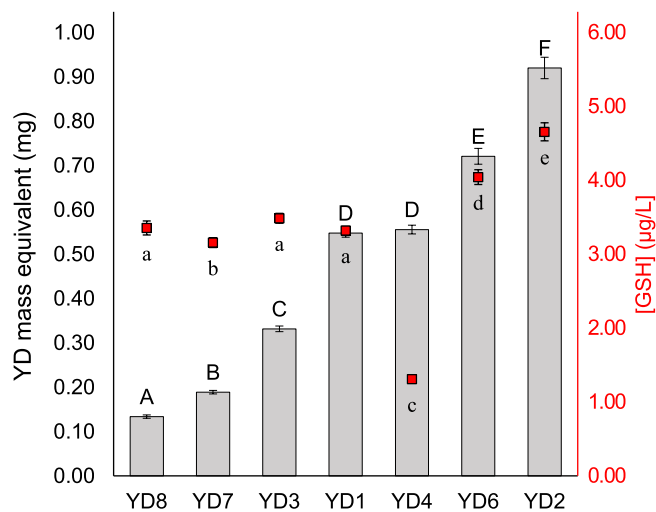


Fig. 1. Mass of yeast derivatives needed to reduce the initial absorbance of DPPH by 20% (left axis) and the corresponding concentration of glutathione in solution (right axis). Different letters represent significant differences after pairwise Wilcoxon test: $n = 6$ and p -value < 0.01.

(Jaehrig et al., 2008). In that assay, insoluble fractions were removed to prevent the adsorption of DPPH on cell walls and consequently reduce the concentration (and absorbance) of the radical, which would lead to an overestimation of the antiradical activity of YDs.

YD6 which was obtained from the same yeast strain as YD7 (strain B) but without the process leading to GSH accumulation in the intracellular medium, exhibited a 3.8 times lower antiradical activity than that of YD7. The antiradical capacity of YD soluble fractions was related not only to the GSH enrichment industrial process, but also to the yeast strain used. Thus, YD1 (strain A) and YD2 (strain B), which were produced without GSH enrichment exhibited significantly different antiradical scavenging activities, with YD1 being more efficient than YD2. It is also interesting to note the biological variability apparent between YD6 and YD2 obtained from the same strain (B) and the same procedure but in different batches. YD6 was significantly more efficient than YD2 (0.72 mg against 0.92 mg respectively) indicating that the technology used to produce the inactive yeast (inactivation procedure, drying system for example) may influence the final activity of the product.

To estimate the impact of the GSH concentration on the DPPH results, it was possible to quantify the concentration of GSH in each YD soluble fraction during the assay (red square in Fig. 1). However, there was no clear relationship between the concentration of GSH during the assay and the antiradical activity of the YDs (Spearman correlation $\rho = 0.46$, p -value > 0.3) despite the known antiradical activity of GSH. YD2, which showed the lowest antiradical activity, was the YD with the highest concentration of GSH during the assay. In contrast, considering equivalent amounts of GSH released by YD8, YD3 and YD1 samples, we observed significant differences in their global antiradical capacity. Therefore, these results led to the conclusion that the activity of the whole soluble fraction (and not only GSH) must impact the antiradical capacity of the YDs estimated by DPPH assay and hence should better explain the classification among YDs than GSH alone. This result is in agreement with a previous study comparing GSH, yeast autolysates and wine lees, where the yeast autolysate (200 mg/L GSH equivalent) showed a greater impact on DPPH discoloration than pure GSH at 500 mg/L (Comuzzo et al., 2015). The potential of the non-GSH fraction on wine aroma stability has also highlighted (Andújar-Ortiz, Rodríguez-Bencomo, Moreno-Arribas, Martín-Álvarez, & Pozo-Bayón, 2010; Rodríguez-Bencomo, Andújar-Ortiz, Sánchez-Patán, Moreno-Arribas, & Pozo-Bayon, 2016). Compounds with reducing property such as cysteine-containing compounds could be more abundant than GSH and thus contribute more than GSH to the pool of reductive compounds (Jaehrig & Rohn, 2007; Roussis, Lambropoulos, & Papadopoulou, 2005). GSH is the most abundant non-proteinaceous thiol in yeast, but the accumulation of low concentrations of other sulfhydryl-containing compounds could greatly impact the global reactivity of the matrix against free radicals, or oxidative species (Rodríguez-Bencomo et al., 2014; Roussis, Papadopoulou, & Sakarellos-Daitsiotis, 2010). Therefore, the increasing level of these compounds with the enrichment process could explain the differential activities of YD7 and YD6 (which differ only in the production process) and also the highest antiradical activity of YD3, YD7 and YD8 (Bahut et al., 2019).

3.2. Estimation of molecular nucleophilic fingerprints of YD soluble fractions

To go beyond the DPPH method, which does not provide any molecular information related to the antioxidant activity of YDs, we applied a derivatization procedure proposed by Romanet et al. (2020) with an electrophilic probe specifically designed to mimic oxidants in wine, coupled with mass spectrometry detection. Derivatization procedures for the detection and quantification of specific compounds are commonly used to increase the limit of detection (LOD) of targeted compounds. For wine oxidative stability studies, the 4-methylquinone (4MeQ), obtained by oxidation of 4-methylcatechol (4MeC), has been

used as a model compound for oxidized polyphenols due to its electrophilic carbon site which could be subject to nucleophilic addition in wine (Danilewicz & Wallbridge, 2010; Danilewicz, 2003, 2013). In addition to sulfites, GSH and ascorbic acid, other nucleophilic compounds, such as thiols, amines and polyphenols, can also competitively react with quinones to form nucleophilic addition products (Nikolantonaki, Magiatis, & Waterhouse, 2014; Waterhouse & Laurie, 2006).

The innovative use of untargeted analysis on derivatized and non-derivatized samples enables the detection of nucleophilic compounds specific for wine relevant antioxidants (Inoue et al., 2013; Romanet et al., 2020). Molecular features (m/z pairs and retention time from UHPLC-Q-ToF-MS analyses in both negative and positive ionization modes) were extracted after addition of increasing amounts of 4MeQ in each YD soluble fractions. The reaction of nucleophiles with quinones resulted in the disappearance of the free nucleophiles and the appearance of new products formed after nucleophilic addition. Spearman correlation tests allowed classification of the compounds either as free nucleophiles ($\rho < 0$) or as their addition reaction products ($\rho > 0$). All Spearman correlation scores are given in Supplementary Information 4. The combination of positive and negative ionization modes enabled the detection of 85 compounds significantly impacted by the presence of the 4MeQ and common to at least three tested YDs.

The great majority of the 85 detected features were detected in negative mode (63) and only 10 features were solely detected in positive mode (the other 12 features were also detected in negative mode), which is in agreement with previous results on the efficiency of the negative ionization mode to detect quinone derivatives (Ma et al., 2019). Features corresponding to nucleophilic addition reaction products ($\rho > 0$) represented the majority of the detected compounds in both positive (73% (16/22)) and negative ionization modes (83% (52/63)). Since the addition reaction products correspond to 4MeC addition on nucleophiles, the diversity of these products is related to the diversity of free nucleophiles, which means that the products of nucleophilic addition are representative of the diversity of nucleophiles present in the solution. The large abundance/diversity of quinone derivatives compared to the few free nucleophiles actually detected illustrates the potential of the proposed derivatization method to improve detection of poorly ionizable free nucleophilic compounds. With respect to these observations, quinone derivatives detected in negative mode were selected as representatives of the nucleophilic fraction (nucleophilic fingerprint, Fig. 2) of the samples and used for further investigation.

These 52 nucleophiles enabled the discrimination of the YDs according to their initial nucleophilic fingerprint and thus their potential antioxidant activity. As previously reported, YD4 appeared chemically significantly different from the others with few nucleophiles (26 detected) at low abundance. Besides YD4, three clusters were clearly defined: YD7-YD8, YD1-YD3 and YD6-YD2. The absolute number of nucleophiles was equivalent (average of 42 ± 2 compounds) between these YDs, but they showed important molecular diversity. Besides the 26 common nucleophiles shared by YD7-YD8, YD1-YD3 and YD6-YD2, 16 compounds were specific to some of these YDs. The chemical proximity between the YD nucleophilic fingerprints is relevant information to attribute similar antioxidant activities to similar samples. In order to estimate this parameter, the principal components analysis of the nucleophilic fingerprint features was performed to reduce the number of dimensions of the data and get an overview of the sample's distance (Fig. 3). In that case, the nucleophilic fingerprint allowed the hierarchization of YDs consistent with that obtained from the DPPH assay.

The DPPH assay revealed the failure of the GSH concentration to explain the scavenging activity of YDs soluble fractions. However, the derivatization procedure highlighted the potential of nucleophiles that were unconsidered until now, to better characterize the antiradical activity of YD soluble fractions. This study showed the major

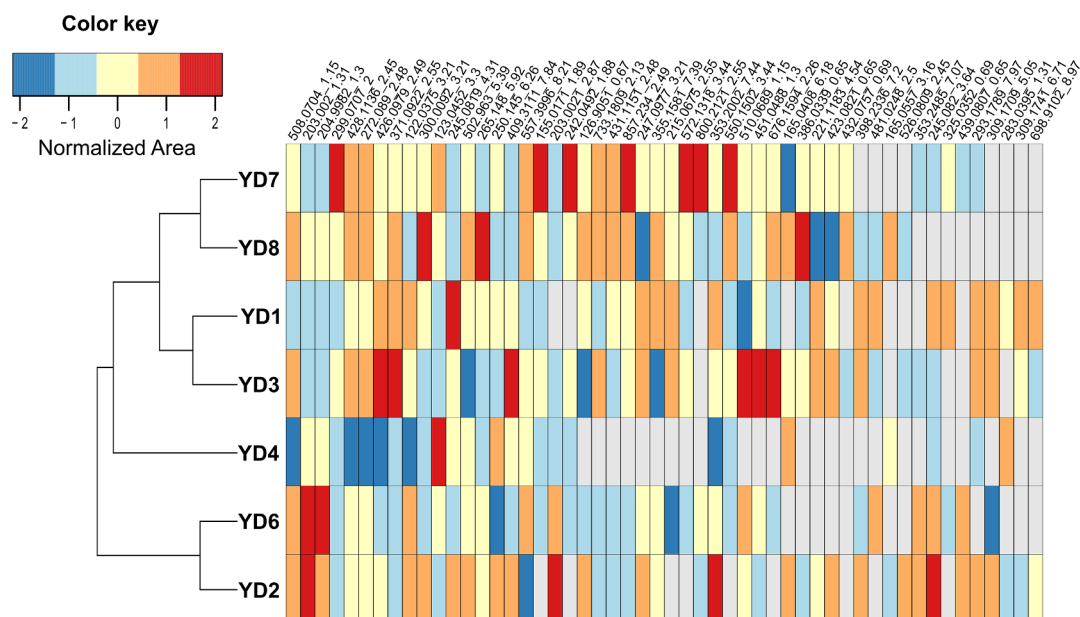


Fig. 2. Heatmap of the nucleophilic fingerprint of yeast derivatives (YDs). Clustering of YDs based on the Euclidean distances between samples. Columns correspond to variables (named as “ m/z _retention time (min)”) significantly increased after the addition of 4-methylquinone (Kruskal-Wallis test, $n = 3$, p -value < 0.05). Grey color represents undetected compounds for a given YD.

importance of the non-targeted approach to consider the global nucleophilic fingerprint for a better assessment of the antioxidant potential of YD soluble fractions. In the present case, the correlation circle plots revealed the features which specifically discriminate the different YDs and pointed out the most relevant (out of the inner circle representing a correlation of 0.8).

In addition to the nucleophilic fingerprint, the high resolution of the UHPLC–Q-ToF-MS has been used to putatively annotate the nucleophiles. Based on the derivatization method, the nucleophilic addition reaction could occur between one or several nucleophiles with one or two electrophilic sites of the 4MeQ (Ma et al., 2019; Nikolantonaki & Waterhouse, 2012; Nikolantonaki et al., 2012, 2014; Romanet et al.,

2020). Table 1 summarizes the putative annotations of the quinone derivatives detected in negative ionization mode, which were positively correlated to the addition of 4MeQ.

Almost 60% (26/44) of the nucleophiles detected were not found in online databases, whatever the combination of 4MeC or HSO₃–4MeC used. Of the 41 attributed elemental formulas, 21 could be putatively assigned to sulfur containing compounds.

Within the annotated adducts, eight were related to GSH or GSH precursors such as cysteine (C₃H₇NO₂S, $m/z = 120.0125$) and glutamyl–cysteine (C₈H₁₄N₂O₅S, $m/z = 249.0551$): [(Cysteine–4MeC–2H)–H][–] (C₁₀H₁₂NO₄S, $m/z = 242.0492$), [(Cys–Gly + 4MeC–2H)–H][–] (C₁₂H₁₅N₂O₅S, $m/z = 299.0707$), [(Glu–

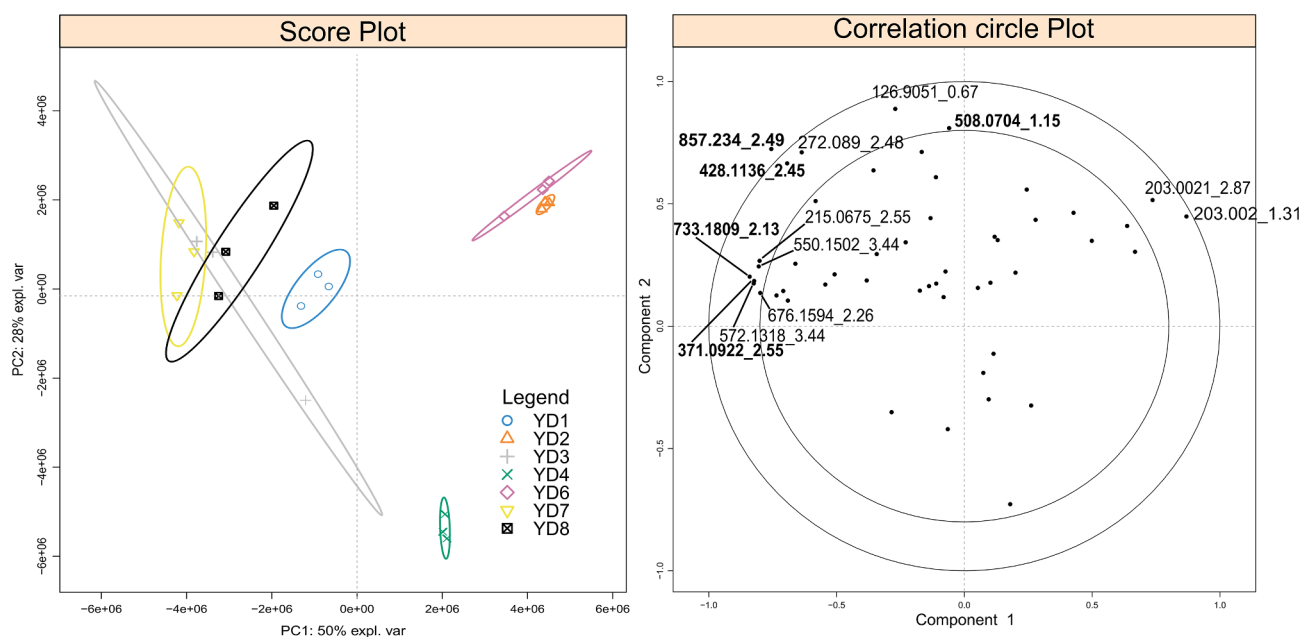


Fig. 3. PCA analysis (scores plot and correlation circle plot) of YD soluble fraction nucleophilic fingerprints. The inner circle in the correlation circle plot corresponds to the correlation at 0.8. Variables are named as “ m/z _retention time (min)”. The ellipse represents confidence level at 95%. Variables in bold are glutathione ([428.1136_2.45], [508.0704_1.15], [733.1809_2.13], [857.234_2.49]) or glutamyl–cysteine ([371.0922_2.55]) quinone addition products ($m^*Nu + n^*4MeC$).

Table 1

Relevant nucleophiles detected in negative ionization mode and their putative annotation based on mass precision and isotopic profiles. The isotopic profile and the MS² profile are available in [Supplementary Information 5](#) for compounds detected with relative intensities higher than 1000. Mono and di-deprotonated free forms of 4-methylcatechol C₇H₇O₂ (*m/z* = 123.0452) and C₇H₆O₂ (*m/z* = 122.0375) respectively as well as the auto-polymerization products C₁₄H₁₃O₄ (*m/z* = 245.0819) and C₁₄H₁₃O₄ (*m/z* = 247.0977) were excluded from the data mining.

<i>m/z</i> _{experimental}	RT	Ion putative formula	Δppm	Adduct	[M]	[M] neutral Formula	YMDB ID	Annotation*
155.0171	1.9	C ₇ H ₇ O ₂ S	-0.80	[(M + 4MeC-2H)-H] ⁻	33.9877	H ₂ S	YMDB00653	hydrogen sulfide
165.0557	3.2	C ₉ H ₉ O ₃	-0.11	[(M + 4MeC-2H)-H] ⁻	44.0262	C ₂ H ₄ O	YMDB00022	acetaldehyde
203.002	1.3	C ₇ H ₇ O ₅ S	0.16	[(M + 4MeC-2H)-H] ⁻	81.9725	H ₂ SO ₃	YMDB00114	sulfite*
203.0021	2.9	C ₇ H ₇ O ₅ S	0.65	[(M + 4MeC-2H)-H] ⁻	81.9725	H ₂ SO ₃	YMDB00114	sulfite
215.0675	2.6	C ₈ H ₁₁ N ₂ O ₅	0.72	[(M + 4MeC-2H)-H] ⁻	94.0378	CH ₆ N ₂ O ₃	-	unknown
221.1183	4.5	C ₁₃ H ₁₇ O ₃	-0.08	[(M + 4MeC-2H)-H] ⁻	100.0888	C ₆ H ₁₂ O	YMDB16016	hexanal*
242.0492	1.9	C ₁₀ H ₁₂ NO ₄ S	-0.21	[(M + 4MeC-2H)-H] ⁻	121.0197	C ₃ H ₇ NO ₂ S	YMDB00046	cysteine
250.145	6.3	C ₁₄ H ₂₀ NO ₃	0.53	[(M + 4MeC-2H)-H] ⁻	129.1154	C ₇ H ₁₅ NO	YMDB16052	isopentylacetamide*
265.148	5.9	C ₁₂ H ₂₅ O ₄ S	0.36	[(M + 4MeC-2H)-H] ⁻	142.1028	C ₅ H ₁₈ O ₂ S	-	unknown
272.089	2.5	C ₁₀ H ₁₄ N ₃ O ₆	0.70	[(M + 4MeC-2H)-H] ⁻	151.0593	C ₂ H ₃ N ₃ O ₄	-	unknown
283.0395	1.3	C ₁₁ H ₁₁ N ₂ O ₅ S	0.30	[(M + 4MeC-2H)-H] ⁻	162.0099	C ₄ H ₆ N ₂ O ₃ S	-	unknown
293.1789	8.0	C ₁₄ H ₂₉ O ₄ S	-1.04	[(M + 4MeC-2H)-H] ⁻	172.1497	C ₇ H ₂₄ O ₂ S	-	unknown
299.0707	2.0	C ₁₂ H ₁₅ N ₂ O ₅ S	-0.05	[(M + 4MeC-2H)-H] ⁻	178.0412	C ₅ H ₁₀ N ₂ O ₃ S	YMDB00690	Cys-Gly
300.0092	3.2	C ₁₃ H ₁₆ N ₃ O ₄ S	2.50	[(M + 4MeC-2H)-H] ⁻	178.9789	C ₆ HN ₃ O ₂ S	-	unknown*
309.1709	5.1	C ₁₇ H ₂₅ O ₅	0.49	[(M + 4MeC-2H)-H] ⁻	188.1412	C ₁₀ H ₂₀ O ₃	YMDB16207	hydroxydecanoic acid
309.1741	6.7	C ₁₄ H ₂₉ O ₅ S	-0.06	[(M + 4MeC-2H)-H] ⁻	216.1508	C ₇ H ₂₄ N ₂ O ₃ S	-	unknown
325.0352	0.7	C ₉ H ₁₃ N ₂ O ₉ S	1.46	[(M + 4MeC + H ₂ SO ₃ -4H)-H] ⁻	124.0484	C ₂ H ₃ N ₂ O ₄	-	unknown
353.2002	7.4	C ₁₆ H ₂₃ O ₆ S	-0.38	[(M + 4MeC-2H)-H] ⁻	232.1708	C ₉ H ₂₈ O ₄ S	-	unknown
353.2485	7.1	C ₁₆ H ₃₇ N ₂ O ₄ S	1.55	[(M + 4MeC-2H)-H] ⁻	232.2184	C ₉ H ₃₂ N ₂ O ₂ S	-	unknown
355.1581	7.4	C ₁₈ H ₂₇ O ₅ S	-1.04	[(M + 4MeC-2H)-H] ⁻	234.1290	C ₁₁ H ₂₂ O ₃ S	-	unknown*
371.0922	2.6	C ₁₅ H ₁₉ N ₂ O ₇ S	0.95	[(M + 4MeC-2H)-H] ⁻	250.0623	C ₈ H ₁₄ N ₂ O ₅ S	YMDB00252	Glu-Cys*
386.0339	0.7	C ₁₀ H ₁₆ N ₃ O ₉ S ₂	1.44	[(M + 4MeC + H ₂ SO ₃ -4H)-H] ⁻	185.0470	C ₃ H ₁₁ N ₃ O ₄ S	-	unknown
398.2336	7.2	C ₂₄ H ₃₂ NO ₄	-0.21	[(M + 4MeC-2H)-H] ⁻	277.2042	C ₁₇ H ₂₇ NO ₂	-	unknown
409.3111	7.8	C ₂₈ H ₄₁ O ₂	-0.25	[(M + 4MeC-2H)-H] ⁻	288.2777	C ₂₁ H ₃₆	-	unknown
423.0821	0.7	C ₁₃ H ₁₉ N ₄ O ₁₀ S	-1.51	[(M + 4MeC + H ₂ SO ₃ -4H)-H] ⁻	302.0505	C ₆ H ₁₄ N ₄ O ₅	-	unknown*
426.0979	2.5	C ₁₈ H ₁₆ N ₇ O ₄ S	-2.57	[(M + 4MeC-2H)-H] ⁻	305.0695	C ₁₁ H ₁₁ N ₇ O ₂ S	-	unknown
428.1136	2.5	C ₁₇ H ₂₂ N ₃ O ₈ S	0.68	[(M + 4MeC-2H)-H] ⁻	307.0838	C ₁₀ H ₁₇ N ₃ O ₆ S	YMDB00160	glutathione*
431.1151	2.5	C ₁₀ H ₁₅ N ₁₂ O ₈	2.25	[(M + 4MeC-2H)-H] ⁻	310.0846	C ₃ H ₁₀ N ₁₂ O ₆	-	unknown
432.0757	0.7	C ₁₂ H ₂₂ N ₃ O ₁₀ S ₂	1.14	[(M + 4MeC + H ₂ SO ₃ -4H)-H] ⁻	231.0889	C ₅ H ₁₇ N ₃ O ₅ S	-	unknown
439.0807	0.7	C ₁₃ H ₁₉ N ₄ O ₁₁ S	-0.74	[(M + 4MeC + H ₂ SO ₃ -4H)-H] ⁻	318.0481	C ₃ H ₁₈ N ₄ O ₆ S	-	unknown
451.0488	1.3	C ₁₅ H ₁₉ N ₂ O ₁₀ S ₂	0.31	[(M + 4MeC + H ₂ SO ₃ -4H)-H] ⁻	250.0623	C ₈ H ₁₄ N ₂ O ₅ S	YMDB00252	Glu-Cys*
481.0248	2.5	C ₂₃ H ₃₁ O ₁₀ S	2.72	[(M + 4MeC + H ₂ SO ₃ -4H)-H] ⁻	290.1154	C ₁₆ H ₁₈ O ₅	-	unknown
502.963	5.4	C ₁₅ H ₁₁ N ₄ O ₁₀ S ₃	-2.54	[(M + 4MeC-2H)-H] ⁻	381.9348	C ₈ H ₆ N ₄ O ₆ S ₃	-	unknown
508.0704	1.2	C ₁₇ H ₂₂ N ₃ O ₁₁ S ₂	0.54	[(M + 4MeC + H ₂ SO ₃ -4H)-H] ⁻	307.0838	C ₁₀ H ₁₇ O ₆ N ₃ S ₁	YMDB00160	glutathione*
526.0809	2.5	C ₁₈ H ₂₀ N ₇ O ₈ S ₂	-2.14	[(M + 4MeC-2H)-H] ⁻	405.0525	C ₁₁ H ₁₅ N ₇ O ₆ S ₂	-	unknown
550.1502	3.4	C ₂₄ H ₂₈ N ₃ O ₁₀ S	0.20	[(M + 4MeC + H ₂ SO ₃ -4H)-H] ⁻	349.1638	C ₁₇ H ₂₃ N ₃ O ₅	Metlin_17974	Tyr-Pro-Ala*
572.1318	3.4	C ₂₂ H ₂₂ N ₉ O ₈ S	0.08	[(M + 4MeC-2H)-H] ⁻	451.1023	C ₁₅ H ₁₇ N ₉ O ₆ S	-	unknown
676.1594	2.3	C ₂₅ H ₃₄ N ₅ O ₁₃ S ₂	-0.89	[(M + 4MeC + H ₂ SO ₃ -4H)-H] ⁻	475.1737	C ₁₈ H ₂₉ N ₅ O ₈ S	200142	Pro-Cys-Gln-Glu
733.1809	2.1	C ₂₇ H ₃₇ N ₆ O ₁₄ S ₂	-0.77	[(M + 4MeC-2H)-H] ⁻	307.0838	C ₁₀ H ₁₇ N ₃ O ₆ S	YMDB00160	glutathione
800.2121	2.6	C ₂₄ H ₃₈ N ₁₁ O ₁₈ S	-0.18	[(M + 4MeC-2H)-H] ⁻	679.1827	C ₁₇ H ₃₃ N ₁₁ O ₁₆ S	-	unknown
857.234	2.5	C ₃₄ H ₄₅ N ₆ O ₁₆ S ₂	0.12	2[(M + 4MeC-2H)-H] ⁻	858.2418	C ₁₀ H ₁₇ N ₃ O ₆ S	YMDB00160	glutathione*

Δppm is calculated as: $\frac{m/z_{\text{experimental}} - m/z_{\text{theoretical}}}{m/z_{\text{theoretical}}} \times 10^6$; *m/z*_{theoretical} corresponds to the exact *m/z* of the ion putative formula.

*Features for which MS/MS profile is provided in supplementary information 5.

Cys + 4MeC-2H-H]⁻ (C₁₅H₁₉N₂O₇S, *m/z* = 371.0922), [(GSH + 4MeC-2H)-H]⁻ (C₁₇H₂₂N₃O₈S, *m/z* = 428.1136), [(Glu-Cys + 4MeC + H₂SO₃-4H)-H]⁻ (C₁₅H₁₉N₂O₁₀S₂, *m/z* = 451.0488), [(GSH + 4MeC + H₂SO₃-4H)-H]⁻ (C₁₇H₂₂N₃O₁₁S₂, *m/z* = 508.0704), [2(GSH + 4MeC-2H)-H]⁻ (C₂₇H₃₇N₆O₁₄S₂, *m/z* = 733.1809) and 2[(GSH + 4MeC-2H)-H]⁻ (C₃₄H₄₅N₆O₁₆S₂, *m/z* = 857.234_2.49). This agrees with the nature of the YDs, since three of these products had been produced in order to accumulate GSH (YD3, YD7 and YD8). The high concentration of GSH and its precursors could explain the abundance of adducts containing these specific nucleophiles. This observation was also corroborated by the correlation circle plot in [Fig. 3](#) where the separation between YD3, YD7 and YD8 is strongly correlated ($\rho > 0.8$) to the abundance of [371.0922_2.55] and [733.1809_2.13], which correspond to Glu-Cys and GSH derivatives, respectively, and to a lower extent to [428.1136_2.45] and [857.234_2.49], which also correspond to GSH derivatives. In [Fig. 3](#), the opposite direction is driven by the abundance of sulfite derivatives [203.0021_2.87] and [203.0020_1.31] in the samples YD2 and YD6. These two compounds correspond to sulfite addition on 4MeC, likely in different C electrophilic sites. The nucleophilic addition of SO₂ is known to be minor in comparison with the reduction of the quinone

(11% yield against 89%, respectively) ([Nikolantonaki & Waterhouse, 2012](#)). Thus, the abundance of sulfonated 4MeC could provide relative information about the underivatized fraction of the 4MeC.

Besides the GSH and GSH precursor derivatives, few other compounds had been annotated from online databases. Notably two peptides Tyr-Pro-Ala (C₂₄H₂₈N₃O₁₀S, *m/z* = 550.1502) and Pro-Cys-Gln-Glu (C₂₅H₃₄N₅O₁₃S₂, *m/z* = 676.1594), which were strongly correlated with the abundance of glutamyl-cysteine and GSH derivatives ([Fig. 3](#)). The correlation between two compounds could indicate the co-accumulation of these peptides during the GSH accumulation process, or the degradation product coming from specific macromolecules involved in the GSH accumulation process. The nucleophilic property of these peptides highlights the wider effect of the GSH enrichment process on a diversity of other metabolites. The quality of the growing environment, notably nutritious factors, is known to impact the genome expression and thus the metabolome of yeasts ([Kresnowati et al., 2006](#)). During the industrial process, this leads to the accumulation of specific metabolites, such as reduced GSH. It was shown that the transient presence of specific nutrients in the yeast culture media can produce yeast with distinct growth and compositional characteristics ([Alfara, Miura, Shimizu, Shioya, & Suga, 1992](#)). Moreover, it was recently shown that

the accumulation of GSH in inactivated *Saccharomyces cerevisiae* yeasts is associated with an increased production of multiple cysteine-containing peptides and other sulfur containing compounds. Finally, Table 1 shows that 13 nucleophiles were formed with compounds which do not contain sulfur. This further indicates the clear potential of chemical families other than thiols to contribute to the antiradical activity of YDs. For example, aldehydes such as acetaldehyde (C_2H_4O , $m/z = 165.0557$) and hexanal ($C_6H_{12}O$, $m/z = 221.1183$) had been annotated as potential 4MeQ binders. These results are in accordance with those found previously in wine, where the reaction between aldehydes and polyphenols is a major step in pigments formation (Li et al., 2008; Oliveira, Ferreira, De Freitas, & Silva, 2011; Waterhouse & Laurie, 2006).

3.3. The role of soluble fraction of YDs on chemically initiated oxidation under wine-like conditions

If the derivatization procedure provided the total relevant nucleophiles present in the solution, which were able to react with an excess concentration of quinone, it must be considered that the oxidation of catechol into quinone is a gradual process catalyzed by metal transition. During this slow oxidation, distinct nucleophiles do not have the same affinity towards the quinone and thus are submitted to competitive additional reactions (Nikolantonaki & Waterhouse, 2012; Nikolantonaki et al., 2012, 2014). Under chemical oxidation conditions in wine-like medium, the oxidation reaction rate is related to the rate of reactive oxygen species formation via the oxidation of polyphenols catalyzed by the presence of metals (Danilewicz, Seccombe, & Whelan, 2008; Elias & Waterhouse, 2010).

In order to investigate the reactivity of YDs under chemical oxidation conditions, YD2, YD3 and YD8 soluble fractions, selected for their low, medium and high nucleophilicity (respectively), according to the different clusters shown Fig. 2 and their antiradical properties (Fig. 1), were submitted to chemical oxidation in the presence of a model polyphenol (4MeC) and of Fe^{2+} . Reactions were conducted at 30 °C and monitored over 40 h, with data collection every 50 min, and then processed to identify nucleophiles strongly correlated with oxidation (Spearman correlation, $\rho \geq |0.85|$). For each m/z -retention time couple, the peak area was centered on its initial value (time = 5 min) and divided by the standard deviation for behavior comparison on a common scale. Fig. 4 represents the evolution of five features during chemical oxidation, considered as representative for kinetic profiles of all detected features.

The production of the oxidant (4MeQ) begins immediately after mixing Fe^{2+} and 4MeC. The rapid increase of GSH-4MeC in the three YDs shows that the 4MeQ was quickly quenched by the GSH which decreased gradually in parallel. After 20 h of oxidation, the free GSH in YD2 is completely depleted while GSH-4MeC reaches a plateau. In contrast, GSH consumption in YD3 and YD8 was not complete even after 40 h (Supplementary Information 6–8). The observed differences between GSH consumption kinetic rates could be guided by the concentration effect and synergic/antagonistic effects, due to the presence of other compounds competing during its nucleophilic addition reaction with the quinone. Indeed, similar to GSH, the unknown nucleophile $C_8H_{16}N_2O_9S_2$ ($m/z = 347.0232$) specific to YD3 and YD8, was totally depleted in YD3 but not in YD8 after 30 h. These results highlight the importance of the chemical diversity of the nucleophilic fingerprints of the YDs for the comprehension of their antioxidant capacity.

Besides the production of GSH-4MeC, the double addition product GSH-4MeC-GSH (equivalent to $C_{27}H_{37}N_6O_{14}S_2$, $m/z = 733.1805$) was not observed in all samples. It never appeared in YD2 while it appeared with delay in YD3 (after 14 h) and YD8 (after 10 h). The production of GSH-4MeC-GSH can be related to (i) a further oxidation of GSH-4MeC derivatives and (ii) a nucleophilic addition of GSH to this specific electrophile. Thus, the higher the concentration of the GSH-4MeC adduct (and the corresponding oxidized form) and that of the remaining

free GSH, the quicker the onset of the double adduct production. This agrees with the quicker appearance and evolution of this double adduct for YD8 than for YD3, where the concentration of free GSH was initially higher. The feature [299.0706_1.96] (annotated as [(Gly-Cys + 4MeC-2H)-H]⁻) exhibited a particular behavior in this example. In YD2, it quickly increased during the first 13 h, reached a maximum and then decreased until total disappearance 15 h later. This reaction could be explained by the rapid nucleophilic addition of Gly-Cys on 4MeQ until a maximum corresponding to the total derivatization of the Gly-Cys. Then the decrease would be interpreted as a second reaction occurring on the simple adduct, such as a second nucleophile addition on the Gly-Cys-4MeC. It is also interesting to note the highly different kinetic of appearance of the Gly-Cys-4MeC. In YD2, the reaction was fast and led to the total derivatization of Gly-Cys, whereas in YD3 and YD8 the reaction occurred with delay and was slow. The presence of competitive reactions for nucleophilic addition could explain these differences as already reported in the literature (Nikolantonaki et al., 2014). Nucleophilic competition can therefore actively modulate the production rate of specific quinone adducts and thus modulate the final chemistry of the wine.

In order to semi-quantify the nucleophilic potential of YDs soluble fractions, the reaction rates of GSH consumption and GSH-4MeC production were calculated directly in their native complex chemical environments. To that purpose, first order kinetic (Eq. (1)) was used to express GSH and GSH-4MeC reaction rates during oxidation:

$$A(t) = A_0 + B * e^{-R*t} \quad (1)$$

With the following constants:

- $A(t)$: Area at time t (a.u.)
- A_0 : Area offset (a.u.)
- B : Initial Area (a.u.)
- R : Rate of the reaction (h^{-1})
- t : time of oxidation (h)

Table 2 presents the fitting parameters for the curves of GSH consumption and GSH-4MeC production for YD2, YD3 and YD8, using Eq. (1). Extensive results such as fitted curves for all replicates and residuals plots are available in Supplementary Information 9–11. The fit with a first order equation matched well with the GSH raw data (adjusted $R^2 > 0.98$ for all replicates). This indicates that the nucleophilic addition of GSH to 4MeQ must be the main reaction leading to the consumption of GSH. In contrast, the production of GSH-4MeC seemed more complex. Since GSH-4MeC-GSH was found in YD3 and YD8, it showed that an equilibrium exists between the GSH-4MeC increase (nucleophilic addition of GSH on 4MeQ) and GSH-4MeC decrease by further nucleophilic addition (for example, nucleophilic addition of GSH on GSH-4MeQ to form GSH-4MeC-GSH present in YD3 and YD8). In the latter reaction, GSH could be replaced by any other nucleophile present in the solution. The apparent first order of the reaction actually hides a complex balance between the appearance of GSH-4MeC and the disappearance of this compound in further reactions. For example, the progressive disappearance of GSH-4MeC is clearly visible in YD2 (Fig. 4) after 20 h. On the basis of these few acknowledged reaction pathways for GSH, we only considered the GSH kinetics for further analysis. The kinetic rate of GSH given by the R parameter in Eq. (1) indirectly estimates the dynamic of reactions occurring in the solution between this compound and its chemical environment.

Parameters A_0 and B give information about the initial and final area of the compound, while R is representative of the global rate of the reaction. In order to compare the rates of reaction between YDs, the half-life constants ($t_{1/2}$, time needed to achieve 50% of the reaction) were calculated as follows (Eq. (2)):

$$t_{1/2} = \frac{\ln(2)}{R} \quad (2)$$

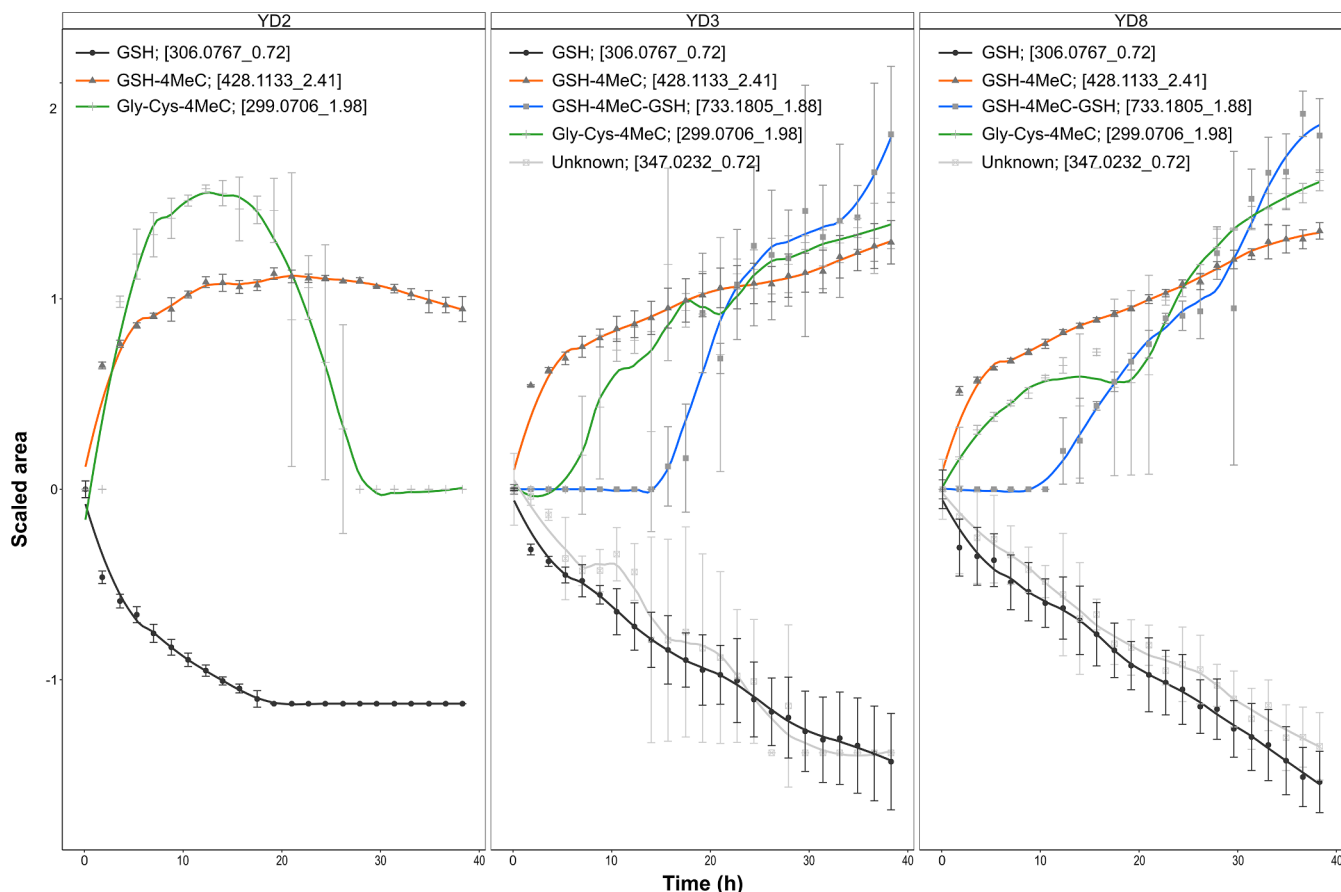


Fig. 4. Representative kinetic profiles of nucleophiles consumption and nucleophile derivatives production under chemical oxidation conditions (4MeC, Fe^{2+} , $30\text{ }^{\circ}\text{C}$) during 40 h. Each point represents the average of three replicates minus the average of the replicates at the initial time of the oxidation, divided by the standard deviation (represented with the error bars). Lines correspond to smoothed values of the area (calculated by Loess method).

YD2 was the only sample where GSH reached total depletion, which gave access to the experimental $t_{1/2}$. The $t_{1/2}$ was estimated to be 4.6 h (Eq. (2)) with the fit, whereas the experimental value was 3.2 ± 0.3 h. The estimation is thus close to the experimental $t_{1/2}$ which consolidates the validity of first order kinetics to estimate the rate of the reaction. Consumption of GSH is significantly quicker for YD2 with a $t_{1/2}$ fifteen and five times lower than YD8 and YD3, respectively.

These results suggest that compounds present in YD samples can interfere with the oxidative chain reaction, normally leading to the reaction of GSH with 4MeQ to produce GSH-4MeC, through possibly more kinetically favorable reactions. Our study enabled us to appreciate the influence of these reactions by tracing the kinetics of GSH

consumption. GSH can be used as an indirect marker to estimate the activity of the pool of nucleophiles to preserve GSH itself. Indeed, the slower kinetic of consumption of GSH (YD8) would be the result of a matrix able to strengthen the action of GSH and thus to preserve this oxidation-sensitive compound. Samples with higher diversity and abundance of nucleophiles (YD3 and YD8) present longer $t_{1/2}$ for consumption of GSH and production of the addition product. In this context, YDs can be ordered from the more nucleophilic to the less nucleophilic: YD8 > YD3 > YD2 based on their $t_{1/2}$. The low abundance of additional nucleophiles in YD2 led to a rapid decrease of GSH until total depletion. YD3 and YD8 released much more GSH in solution compared to YD2 and did not reach the plateau after 40 h of oxidation.

Table 2

Parameters of the first order fit (Eq. (1)) and associated half-life time ($t_{1/2}$) and adjusted R^2 . Different letters represent significant differences after Wilcoxon test, $n = 3$ and p -value < 0.05.

GSH					
	A_0 (a.u.)	B (a.u.)	R (h^{-1})	$t_{1/2}$ (h)	adj. R^2
YD2	$-9.8 \times 10^3 \pm 4.4 \times 10^3$ a	$5.9 \times 10^5 \pm 2.7 \times 10^4$ a	0.15 ± 0.01 a	4.6	0.98
YD3	$-3.1 \times 10^3 \pm 2.3 \times 10^5$ a	$1.4 \times 10^6 \pm 2.5 \times 10^5$ ab	0.03 ± 0 ab	23.1	0.98
YD8	$-1.5 \times 10^6 \pm 7.8 \times 10^5$ a	$4.0 \times 10^6 \pm 8.2 \times 10^5$ b	0.01 ± 0 b	69.3	0.99
GSH-4MeC					
	A_0 (a.u.)	B (a.u.)	R (h^{-1})	$t_{1/2}$ (h)	adj. R^2
YD2	$2.6 \times 10^6 \pm 3.9 \times 10^4$ a	$-2.1 \times 10^6 \pm 1.1 \times 10^5$ a	0.36 ± 0.01 a	1.9	0.88
YD3	$3.4 \times 10^6 \pm 3.2 \times 10^5$ ab	$-2.3 \times 10^6 \pm 3.4 \times 10^4$ a	0.07 ± 0.02 ab	9.9	0.92
YD8	$4.9 \times 10^6 \pm 1.4 \times 10^5$ b	$-3.7 \times 10^6 \pm 1.7 \times 10^5$ a	0.03 ± 0 b	23.1	0.94

But interestingly, they exhibited high differences in $t_{1/2}$. Associated with the higher amount of GSH, YD8 exhibited a slower (but not significant at p -value ≤ 0.05) consumption rate than YD3. This shows that independently of the concentration of GSH, the co-accumulated nucleophiles effectively preserve the pool of GSH. This result is in accordance with our previous results showing the positive impact of the GSH accumulation process on the quality and quantity of potential nucleophilic compounds (Bahut et al., 2019).

In addition, this nucleophilic order (YD8 > YD3 > YD2) order matches perfectly with the antiradical activity of these samples found with the DPPH assay. The DPPH assay demonstrates that GSH alone does not allow characterization of the antiradical activity of YDs (Comuzzo et al., 2015). But here, the observation of the activity of the other nucleophilic compounds allows better understanding of the potential pool of compounds behind the antiradical activity. These results put emphasis on the significance of a complex pool of nucleophilic compounds, rarely considered so far, which contributes to the overall antioxidant activity of samples such as YDs.

4. Conclusions

The metabolomics approach provided evidence of specific fingerprints for YD soluble fractions. The DPPH assay of these soluble fractions was performed in order to assess the YD antiradical activity. The higher radical scavenging activity of yeast derivatives naturally rich in GSH pointed out the positive influence of this specific production process on the antioxidant activities of the YDs. Nevertheless, GSH concentrations appeared poorly correlated with the DPPH scores implying the potential contribution of a larger pool of compounds from YDs to the oxidative stability. The use of a model electrophile (4-methyl-1,2-benzoquinone) as a derivatization agent revealed a pool of nucleophiles which may react with quinones in model wine; 52 nucleophiles discriminated the YDs into four groups based on the number and the abundance of these reactive compounds. This innovative separation of samples only based on derivatized compounds matched very well with the DPPH scores, allowing samples to be ordered based on their stabilizing activity: YD8 > YD7 > YD3 > YD1 > YD4 > YD6 > YD2. The UHPLC-Q-ToF-MS further enabled annotation of most of the nucleophiles, which mostly belong to sulfur and nitrogen-sulfur compounds. Our results confirmed the need to consider the whole chemical diversity of the nucleophilic fraction present in the sample, beyond the sole GSH concentration. However, monitoring the consumption rate of specific nucleophiles (for example GSH) can be used as an indirect marker to estimate the activity of the entire pool of nucleophiles. Indeed, YDs with the highest number of kinetically favorable nucleophilic reactions (longest GSH half-life in this example) also appeared to possess the best antiradical activity. The important issue for the practical application of GSH-enriched YDs in wine, would thus be that the slower the kinetic rate of the GSH consumption (longer $t_{1/2}$), the higher the YD antioxidant potential, because wine could thus benefit from a long-lasting reservoir of GSH antioxidant. This work opens new perspectives for the analysis and development of yeast preparations dedicated to improving wine oxidative stability.

Declaration of Competing Interest

The authors declare that they have no known competing financial interests or personal relationships that could have appeared to influence the work reported in this paper.

Acknowledgements

The authors acknowledge the Regional Council of Bourgogne – Franche-Comté, the “Fonds Européen de Développement Régional (FEDER)” and Lallemand SA (31, Blagnac) for financial support. The authors would like to thank Lallemand SA (31) and Oenobrand (34) for

the yeast derivatives supply. They also would like to thank Dr. Eveline Bartowsky for a careful reading of the manuscript by a native English speaker.

Appendix A. Supplementary data

Supplementary data to this article can be found online at <https://doi.org/10.1016/j.foodchem.2020.126941>.

References

- Alfara, C. G., Miura, K., Shimizu, H., Shioya, S., & Suga, K. I. (1992). Cysteine addition strategy for maximum glutathione production in fed-batch culture of *Saccharomyces cerevisiae*. *Applied Microbiology and Biotechnology*, 37(2), 141–146. <https://doi.org/10.1007/BF00178160>.
- Andújar-Ortiz, I., Rodríguez-Bencomo, J. J., Moreno-Arribas, M. V., Martín-Álvarez, P. J., & Pozo-Bayón, M. A. (2010). Role of glutathione enriched inactive yeast preparations. *Instituto de Fermentaciones Industriales CSIC*, 1–8.
- Bahut, F., Liu, Y., Romanet, R., Coelho, C., Sieczkowski, N., Alexandre, H., ... Gougeon, R. D. R. D. (2019). Metabolic diversity conveyed by the process leading to glutathione accumulation in inactivated dry yeast: A synthetic media study. *Food Research International*, 123, 762–770. <https://doi.org/10.1016/j.foodres.2019.06.008>.
- Comuzzo, P., Battistutta, F., Vendrame, M., Páez, M. S., Luisi, G., & Zironi, R. (2015). Antioxidant properties of different products and additives in white wine. *Food Chemistry*, 168, 107–114. <https://doi.org/10.1016/j.foodchem.2014.07.028>.
- Comuzzo, P., Tat, L., Liessi, A., Brotto, L., Battistutta, F., & Zironi, R. (2012). Effect of different lysis treatments on the characteristics of yeast derivatives for winemaking. *Journal of Agricultural and Food Chemistry*, 60(12), 3211–3222. <https://doi.org/10.1021/jf204669f>.
- Danilewicz, J. C. (2003). Review of reaction mechanisms of oxygen and proposed intermediate reduction products in wine: Central role of iron and copper. *American Journal of Enology and Viticulture*, 54(2), 73–85. <http://www.ajevonline.org.ezproxy.lib.calpoly.edu/content/ajev/54/2/73.full.pdf>.
- Danilewicz, J. C. (2013). Reactions involving iron in mediating catechol oxidation in model wine. *American Journal of Enology and Viticulture*, 64(3), 316–324. <https://doi.org/10.5344/ajev.2013.12137>.
- Danilewicz, J. C., Secombe, J. T., & Whelan, J. (2008). Mechanism of interaction of polyphenols, oxygen, and sulfur dioxide in model wine. *American Journal of Enology and Viticulture*, 59(2), 128–136. <https://doi.org/10.1680/istbu.1995.27310>.
- Danilewicz, J. C., & Wallbridge, P. J. (2010). Further studies on the mechanism of interaction of polyphenols, oxygen, and sulfite in wine. *American Journal of Enology and Viticulture*, 25(2), 119–126. <https://www.ajevonline.org/content/61/2/166.abstract>.
- Dubourdieu, D., & Lavigne, V. (2004). The role of glutathione on the aromatic evolution of dry white wine. *Vinidea. Net Wine Internet Technical Journal*, 02(2), 1–9. <https://www.infowine.com>.
- Elias, R. J., Andersen, M. L., Skibsted, L. H., Waterhouse, A. L., Ryan, J., Andersen, M. L., ... Waterhouse, A. L. (2009). Key factors affecting radical formation in wine studied by spin trapping and EPR spectroscopy. *American Journal of Enology and Viticulture*, 60(4), 471–476. <https://doi.org/10.1021/jf8035484>.
- Elias, R. J., & Waterhouse, A. L. (2010). Controlling the fenton reaction in wine. *Journal of Agricultural and Food Chemistry*, 58(3), 1699–1707. <https://doi.org/10.1021/jf903127r>.
- Gabrielli, M., Alexandre-Tudo, J. L., Kilmartin, P. A., Sieczkowski, N., & du Toit, W. J. (2017). Additions of glutathione or specific glutathione-rich dry inactivated yeast preparation (DYP) to sauvignon blanc must: Effect on wine chemical and sensory composition. *South African Journal of Enology and Viticulture*, 38(1), 18–28. <https://doi.org/10.21548/38-1-794>.
- Inoue, K., Nishimura, M., Tsutsui, H., Min, J. Z., Todoroki, K., Kauffmann, J. M., & Toyo'oka, T. (2013). Foodomics platform for the assay of thiols in wines with fluorescence derivatization and ultra performance liquid chromatography mass spectrometry using multivariate statistical analysis. *Journal of Agricultural and Food Chemistry*, 61(6), 1228–1234. <https://doi.org/10.1021/jf304822t>.
- Jaehrig, S. C., & Rohn, S. (2007). In Vitro Potential Antioxidant Activity of (1→3), (1→6)-β-d-glucan and Protein Fractions from *Saccharomyces cerevisiae* Cell Walls. *Journal of Agricultural and Food Chemistry*, 55(12), 4710–4716. <https://doi.org/10.1021/jf063209q>.
- Jaehrig, S. C., Rohn, S., Kroh, L. W., Wildenauer, F. X., Lisdat, F., Fleischer, L. G., & Kurz, T. (2008). Antioxidative activity of (1→3), (1→6)-β-d-glucan from *Saccharomyces cerevisiae* grown on different media. *LWT - Food Science and Technology*, 41(5), 868–877. <https://doi.org/10.1016/j.lwt.2007.06.004>.
- Kontogeorgos, N., & Roussis, I. G. (2014). Total free sulphhydryls of several white and red. *South African Journal of Enology and Viticulture*, 35(1), 2013–2015.
- Kreitman, G. Y., Laurie, V. F., & Elias, R. J. (2013). Investigation of ethyl radical quenching by phenolics and thiols in model wine. *Journal of Agricultural and Food Chemistry*, 61(3), 685–692. <https://doi.org/10.1021/jf303880g>.
- Kresnowati, M. T. A. P., Van Winden, W. A., Almering, M. J. H., Ten Pierick, A., Ras, C., Knijnenburg, T. A., ... Daran, J. M. (2006). When transcriptome meets metabolome: Fast cellular responses of yeast to sudden relief of glucose limitation. *Molecular Systems Biology*, 2. <https://doi.org/10.1038/msb4100083>.
- Kritzinger, E. C., Bauer, F. F., & Du Toit, W. J. (2013). Role of glutathione in winemaking: A review. *Journal of Agricultural and Food Chemistry*, 61(2), 269–277. <https://doi.org/10.1021/jf303665z>.

- Li, H., Guo, A., & Wang, H. (2008). Mechanisms of oxidative browning of wine. *Food Chemistry*, 108(1), 1–13. <https://doi.org/10.1016/j.foodchem.2007.10.065>.
- Ma, L., Bueschl, C., Schuhmacher, R., & Waterhouse, A. L. (2019). Tracing oxidation reaction pathways in wine using ¹³C isotopolog patterns and a putative compound database. *Analytica Chimica Acta*, 1054, 74–83. <https://doi.org/10.1016/j.aca.2018.12.019>.
- Nikolantonaki, M., Jourdes, M., Shinoda, K., Teissedre, P.-L., Quideau, S., & Darriet, P. (2012). Identification of adducts between an odoriferous volatile thiol and oxidized grape phenolic compounds: Kinetic study of adduct formation under chemical and enzymatic oxidation conditions. *Journal of Agricultural and Food Chemistry*, 60(10), 2647–2656. <https://doi.org/10.1021/jf204295s>.
- Nikolantonaki, M., Julien, P., Coelho, C., Roullier-Gall, C., Ballester, J., Schmitt-Kopplin, P., & Gougeon, R. D. (2018). Impact of glutathione on wines oxidative stability: A combined sensory and metabolomic study. *Frontiers in Chemistry*, 6(June), 1–9. <https://doi.org/10.3389/fchem.2018.00182>.
- Nikolantonaki, M., Magiatis, P., & Waterhouse, A. L. (2014). Measuring protection of aromatic wine thiols from oxidation by competitive reactions vs wine preservatives with ortho-quinones. *Food Chemistry*, 163, 61–67. <https://doi.org/10.1016/j.foodchem.2014.04.079>.
- Nikolantonaki, M., & Waterhouse, A. L. (2012). A method to quantify quinone reaction rates with wine relevant nucleophiles: A key to the understanding of oxidative loss of varietal thiols. *Journal of Agricultural and Food Chemistry*, 60(34), 8484–8491. <https://doi.org/10.1021/jf302017j>.
- Oliveira, C. M., Ferreira, A. C. S., De Freitas, V., & Silva, A. M. S. S. (2011). Oxidation mechanisms occurring in wines. *Food Research International*, 44(5), 1115–1126. <https://doi.org/10.1016/j.foodres.2011.03.050>.
- Papadopoulou, D., & Roussis, I. G. (2008). Inhibition of the decrease of volatile esters and terpenes during storage of a white wine and a model wine medium by glutathione and N-acetylcysteine. *International Journal of Food Science and Technology*, 43(6), 1053–1057. <https://doi.org/10.1111/j.1365-2621.2007.01562.x>.
- Pozo-Bayon, M.a., Andujar-Ortiz, I., & Moreno-Arribas, M. V. (2009). Scientific evidences beyond the application of inactive dry yeast preparations in winemaking. *Food Research International*, 42(7), 754–761. <https://doi.org/10.1016/j.foodres.2009.03.004>.
- Rodriguez-Bencomo, J. J., Andujar-Ortiz, I., Moreno-Arribas, M. V., Sima, C., Gonzalez, J., Chana, A., ... Pozo-Bayon, M. A. (2014). Impact of glutathione-enriched inactive dry yeast preparations on the stability of terpenes during model wine aging. *Journal of Agricultural and Food Chemistry*, 62(6), 1373–1383. <https://doi.org/10.1021/jf402866q>.
- Rodriguez-Bencomo, J. J., Andujar-Ortiz, I., Sánchez-Patán, F., Moreno-Arribas, M. V., & Pozo-Bayon, M. A. (2016). Fate of the glutathione released from inactive dry yeast preparations during the alcoholic fermentation of white musts. *Australian Journal of Grape and Wine Research*, 22(1), 46–51. <https://doi.org/10.1111/ajgw.12161>.
- Romanet, R., Bahut, F., Nikolantonaki, M., & Gougeon, R. D. (2020). Molecular characterization of white wines antioxidant metabolome by ultra high performance liquid chromatography high-resolution mass spectrometry. *Antioxidants*, 9(2), <https://doi.org/10.3390/antiox9020115>.
- Romanet, R., Coelho, C., Liu, Y., Bahut, F., Ballester, J., Nikolantonaki, M., & Gougeon, R. D. (2019). The antioxidant potential of white wines relies on the chemistry of sulfur-containing compounds: An optimized DPPH assay. *Molecules*, 24(7), 1353. <https://doi.org/10.3390/molecules24071353>.
- Roussis, I. G., Patrianakou, M., & Drossiadis, A. (2013). Protection of aroma volatiles in a red wine with low sulphur dioxide by a mixture of glutathione, caffeic acid and gallic acid. *South African Journal of Enology and Viticulture*, 34(2), 262–265. DOI:10.21548/34-2-1103.
- Roussis, Ioannis G., Lambropoulos, I., & Papadopoulou, D. (2005). Inhibition of the decline of volatile esters and terpenols during oxidative storage of Muscat-white and Xinomavro-red wine by caffeic acid and N-acetyl-cysteine. *Food Chemistry*, 93(3), 485–492. <https://doi.org/10.1016/j.foodchem.2004.10.025>.
- Roussis, Ioannis G., Papadopoulou, D., & Sakarellos-Daitsiotis, M. (2010). Protective effect of thiols on wine aroma volatiles. *The Open Food Science Journal*, 3(1), 98–102. <https://doi.org/10.2174/1874256400903010098>.
- Sonni, F., Moore, E. G., Clark, A. C., Chinnici, F., Riponi, C., & Scollary, G. R. (2011). Impact of glutathione on the formation of methylmethine-and carboxymethine-bridged (+)-catechin dimers in a model wine system. *Journal of Agricultural and Food Chemistry*, 59(13), 7410–7418. <https://doi.org/10.1021/jf200968x>.
- Suhre, K., & Schmitt-Kopplin, P. (2008). MassTRIX: Mass translator into pathways. *Nucleic Acids Research Web Server*, 36, 481–484. <https://doi.org/10.1093/nar/gkn194>.
- Waterhouse, A. L., & Laurie, V. F. (2006). Oxidation of Wine Phenolics: A Critical Evaluation and Hypotheses. *American Journal of Enology and Viticulture*, 57(3), 306–313. <http://www.ajevonline.org/content/57/3/306>.